Received: 27 September 2022 | Accepted: 21 December 2022

DOI: 10.1002/pamm.202200037

A Novel Energy and Momentum Consistent Mixed Formulation for Coupled Nonlinear Electro-Thermo-Elastodynamics

Felix Zähringer[1,*], **Marlon Franke**[1], and **Peter Betsch**[1]

[1] Institute of Mechanics, Karlsruhe Institute of Technology (KIT), Otto-Ammann-Platz 9, 76131 Karlsruhe, Germany

In the present contribution, a novel mixed formulation aimed at the energy-momentum consistent simulation of coupled nonlinear electro-thermo-elastodynamic systems, in particular dielectric elastomer actuators, is proposed. It is essentially based on a mixed framework for elastodynamics in the case of polyconvex stored energy functions. In accordance with this framework, the properties of the rediscovered tensor cross product are exploited in a first step to derive a mixed formulation via a Hu-Washizu type extension of the stored energy function. Afterwards, the corresponding strong form is derived and supplemented with the (initial) boundary value problems of thermodynamics and electrostatics. By additionally choosing an appropriate polyconvexity-inspired energy density function, this procedure leads to a fully coupled electro-thermo-elastodynamic formulation that benefits from the properties of the underlying mixed framework.
Furthermore, an energy-momentum consistent time integration scheme is proposed for the novel framework, where discrete derivatives in the sense of Gonzalez are employed. The formulation is second-order accurate and stable even for large time step sizes. Eventually, the performance of the novel formulation is illustrated in a numerical example.

1 Introduction

Dielectric elastomer actuators (DEAs) are expected to be used in many future applications, especially in the field of soft robotics [1]. Their simplest design is similar to that of a parallel-plate capacitor. More precisely, it consists of two electrodes that are separated by an elastomer layer with notable low stiffness properties. When a voltage is applied between these two electrodes, the so-called Coulomb force takes effect, causing deformation of the elastomer layer. For more sophisticated DEAs, it is reasonable to develop suitable simulation programs that are able to accurately predict their complex actuation characteristics. This includes in particular the consideration of temperature effects. Furthermore, physical conservation laws should be replicated exactly for reliable long term simulations. Therefore, we propose a novel energy and momentum consistent mixed formulation for coupled nonlinear electro-thermo-elastodynamics in our present contribution.

This work is structured as follows. First, in Sec. 2, we present the main fundamentals of our work. Besides a short introduction to the tensor cross product, we outline the key characteristics of a mixed formulation for elastostatics. Second, in Sec. 3, we point out a general way, how mixed mechanical frameworks can be transferred to coupled problems, in particular to electro-thermo-elastodynamics. In addition, we present an energy and momentum consistent temporal discretization and a spatial discretization based on the finite element method. The section is concluded by a numerical example that illustrates the properties of the novel framework. Finally, in Sec. 4, we provide concluding remarks.

2 Fundamentals

In this section, we introduce the tensor cross product and a mixed framework for elastostatics (cf. [3]). The latter serves as a basis for subsequent considerations.

2.1 Tensor cross product

The tensor cross product is a rather unknown algebraic operation that connects two second-order tensors $\mathbf{A}$, $\mathbf{B} \in \mathbb{R}^{3\times3}$. According to [2], the tensor cross product is defined by

$$(\mathbf{A} \boxtimes \mathbf{B})_{ij} = \epsilon_{i\alpha\beta}\, \epsilon_{jab}\, \mathbf{A}_{\alpha a}\, \mathbf{B}_{\beta b}, \tag{1}$$

where ϵ_{ijk} is the third-order permutation tensor. This definition is reminiscent of the cross product between two vectors $\mathbf{a}$, $\mathbf{b} \in \mathbb{R}^3$, given by

$$(\mathbf{a} \times \mathbf{b})_i = \epsilon_{ijk}\, a_j\, b_k. \tag{2}$$

As shown in detail in [3], the cofactor and the determinant of a second-order tensor $\mathbf{A} \in \mathbb{R}^{3\times3}$ can be expressed as

$$\operatorname{cof}(\mathbf{A}) = \tfrac{1}{2}\,(\mathbf{A} \boxtimes \mathbf{A}), \quad \det(\mathbf{A}) = \tfrac{1}{3}\operatorname{cof}(\mathbf{A}) : \mathbf{A} = \tfrac{1}{6}\,(\mathbf{A} \boxtimes \mathbf{A}) : \mathbf{A}, \tag{3}$$

using the tensor cross product. Further useful properties of the tensor cross product can be found, for example, in [4].

* Corresponding author: e-mail felix.zaehringer@kit.edu, phone +49 721 608 43252, fax +49 721 608 47990

2.2 A mixed framework for elastostatics

An elastostatic body $\mathcal{B}_0$ is often described via its potential energy

$$\Pi^{\mathrm{m}}(\boldsymbol{\varphi}) = \Pi^{\mathrm{m,int}}(\boldsymbol{\varphi}) + \Pi^{\mathrm{m,ext}}(\boldsymbol{\varphi}), \tag{4}$$

with

$$\Pi^{\mathrm{m,int}}(\boldsymbol{\varphi}) = \int_{\mathcal{B}_0} W(\mathbf{F}(\boldsymbol{\varphi}))\,\mathrm{d}V, \quad \Pi^{\mathrm{m,ext}}(\boldsymbol{\varphi}) = -\int_{\mathcal{B}_0} \bar{\mathbf{B}}\cdot\boldsymbol{\varphi}\,\mathrm{d}V - \int_{\partial_{\boldsymbol{T}}\mathcal{B}_0} \bar{\mathbf{T}}\cdot\boldsymbol{\varphi}\,\mathrm{d}A. \tag{5}$$

In the above, the internal contribution to the potential energy $\Pi^{\mathrm{m,int}}$ depends on a stored energy function W that is given here as a function of the deformation gradient $\mathbf{F}$ which in turn depends on the displacement field $\boldsymbol{\varphi}$. The external contribution $\Pi^{\mathrm{m,ext}}$ further depends on a prescribed reference body force $\bar{\mathbf{B}}$ acting in the considered body $\mathcal{B}_0$ and the first Piola-Kirchhoff traction vector $\bar{\mathbf{T}}$ given on the boundary of the body $\partial_{\boldsymbol{T}}\mathcal{B}_0$. The first variation of the potential energy (4) with respect to the unknown variable, in this case the displacement field $\boldsymbol{\varphi}$, yields the weak form of the problem

$$\delta_{\boldsymbol{\varphi}}\Pi^{\mathrm{m}} = \int_{\mathcal{B}_0} \partial_{\mathbf{F}} W(\mathbf{F}) : \delta\mathbf{F}\,\mathrm{d}V + \Pi^{\mathrm{m,ext}}(\delta\boldsymbol{\varphi}) = 0. \tag{6}$$

The stored energy function in (5) can alternatively be expressed as

$$W(\mathbf{F}) = \hat{W}(\mathbf{F},\, \mathrm{cof}(\mathbf{F}),\, \det(\mathbf{F})), \tag{7}$$

i.e., as a function of the deformation gradient, its cofactor, and its determinant. If the stored energy function $\hat{W}$ is convex with respect to all of its arguments, it can be referred to as a polyconvex stored energy function [5]. Moreover, if the polyconvex stored energy function $\hat{W}$ satisfies the axiom of frame-indifference, it can be expressed by (cf. [3])

$$W(\mathbf{F}) = \mathbb{W}\left(\mathbf{C},\, \mathbf{G},\, C\right) \tag{8}$$

using the right Cauchy-Green deformation tensor

$$\mathbf{C} = \mathbf{F}^{\mathrm{T}}\mathbf{F} \tag{9}$$

and two additional kinematic quantities

$$\mathbf{G} = \tfrac{1}{2}\mathbf{C}\barwedge\mathbf{C}, \quad C = \tfrac{1}{3}\mathbf{G} : \mathbf{C}. \tag{10}$$

We assume such a polyconvex stored energy function in what follows. It is then possible to re-express the potential energy of an elastostatic system (4) as

$$\begin{aligned}\tilde{\Pi}^{\mathrm{m}}(\boldsymbol{\varphi}, \boldsymbol{\Xi}, \boldsymbol{\Lambda}) = \int_{\mathcal{B}_0} \mathbb{W}\left(\mathbf{C}, \mathbf{G}, C\right) &+ \boldsymbol{\Lambda}^{\mathbf{C}} : \left(\mathbf{F}^{\mathrm{T}}\mathbf{F} - \mathbf{C}\right) \\ &+ \boldsymbol{\Lambda}^{\mathbf{G}} : \left(\tfrac{1}{2}\mathbf{C}\barwedge\mathbf{C} - \mathbf{G}\right) \\ &+ \Lambda^{C}\left(\tfrac{1}{3}\mathbf{G} : \mathbf{C} - C\right)\,\mathrm{d}V + \Pi^{\mathrm{m,ext}}(\boldsymbol{\varphi}).\end{aligned} \tag{11}$$

Therein, the kinematic relations (9)-(10) are enforced via the Lagrange multipliers $\boldsymbol{\Lambda}^{\mathbf{C}}$, $\boldsymbol{\Lambda}^{\mathbf{G}}$, and Λ^{C}. This extended formulation of the potential energy is very similar to the well-known Hu-Washizu principle and now depends not only on the displacement field $\boldsymbol{\varphi}$, but also on the additional kinematic quantities $\boldsymbol{\Xi} = (\mathbf{C}, \mathbf{G}, C)$ and the Lagrange multipliers $\boldsymbol{\Lambda} = (\boldsymbol{\Lambda}^{\mathbf{C}}, \boldsymbol{\Lambda}^{\mathbf{G}}, \Lambda^{C})$. The first variation of this extended potential energy with respect to all independent variables yields

$$\begin{aligned}
\delta_{\boldsymbol{\varphi}}\tilde{\Pi}^{\mathrm{m}} &= \int_{\mathcal{B}_0} \boldsymbol{\Lambda}^{\mathbf{C}} : \left(\delta\mathbf{F}^{\mathrm{T}}\mathbf{F} + \mathbf{F}^{\mathrm{T}}\delta\mathbf{F}\right)\,\mathrm{d}V + \Pi^{\mathrm{ext}}(\delta\boldsymbol{\varphi}) = 0 \\
\delta_{\mathbf{C}}\tilde{\Pi}^{\mathrm{m}} &= \int_{\mathcal{B}_0} \delta\mathbf{C} : \left(\partial_{\mathbf{C}}\mathbb{W} - \boldsymbol{\Lambda}^{\mathbf{C}} + \boldsymbol{\Lambda}^{\mathbf{G}}\barwedge\mathbf{C} + \tfrac{1}{3}\Lambda^{C}\mathbf{G}\right)\,\mathrm{d}V = 0 \\
\delta_{\mathbf{G}}\tilde{\Pi}^{\mathrm{m}} &= \int_{\mathcal{B}_0} \delta\mathbf{G} : \left(\partial_{\mathbf{G}}\mathbb{W} - \boldsymbol{\Lambda}^{\mathbf{G}} + \tfrac{1}{3}\Lambda^{C}\mathbf{C}\right)\,\mathrm{d}V = 0 \\
\delta_{C}\tilde{\Pi}^{\mathrm{m}} &= \int_{\mathcal{B}_0} \delta C\left(\partial_{C}\mathbb{W} - \Lambda^{C}\right)\,\mathrm{d}V = 0 \\
\delta_{\boldsymbol{\Lambda}^{\mathbf{C}}}\tilde{\Pi}^{\mathrm{m}} &= \int_{\mathcal{B}_0} \delta\boldsymbol{\Lambda}^{\mathbf{C}} : \left(\mathbf{F}^{\mathrm{T}}\mathbf{F} - \mathbf{C}\right)\,\mathrm{d}V = 0 \\
\delta_{\boldsymbol{\Lambda}^{\mathbf{G}}}\tilde{\Pi}^{\mathrm{m}} &= \int_{\mathcal{B}_0} \delta\boldsymbol{\Lambda}^{\mathbf{G}} : \left(\tfrac{1}{2}\mathbf{C}\barwedge\mathbf{C} - \mathbf{G}\right)\,\mathrm{d}V = 0 \\
\delta_{\Lambda^{C}}\tilde{\Pi}^{\mathrm{m}} &= \int_{\mathcal{B}_0} \delta\Lambda^{C}\left(\tfrac{1}{3}\mathbf{G} : \mathbf{C} - C\right)\,\mathrm{d}V = 0,
\end{aligned} \tag{12}$$

which is equivalent to the weak form of this mixed elastostatic formulation. Since all variations $\delta(\bullet)$ therein are arbitrary, it is possible to derive the differential or strong form via basic algebraic operations. This strong form consists of the equations

$$\begin{aligned}
&\mathrm{Div}\left(2\mathbf{F}\boldsymbol{\Lambda}^{\mathbf{C}}\right)+\bar{\mathbf{B}}=\mathbf{0} && \text{in } \mathcal{B}_0, && (13a)\\
&\partial_{\mathbf{C}}\mathbb{W}-\boldsymbol{\Lambda}^{\mathbf{C}}+\boldsymbol{\Lambda}^{\mathbf{G}}\divideontimes\mathbf{C}+\tfrac{1}{3}\Lambda^{C}\mathbf{G}=\mathbf{0} && \text{in } \mathcal{B}_0, && (13b)\\
&\partial_{\mathbf{G}}\mathbb{W}-\boldsymbol{\Lambda}^{\mathbf{G}}+\tfrac{1}{3}\Lambda^{C}\mathbf{C}=\mathbf{0} && \text{in } \mathcal{B}_0, && (13c)\\
&\partial_{C}\mathbb{W}-\Lambda^{C}=0 && \text{in } \mathcal{B}_0, && (13d)\\
&\mathbf{F}^{\mathrm{T}}\mathbf{F}-\mathbf{C}=\mathbf{0} && \text{in } \mathcal{B}_0, && (13e)\\
&\tfrac{1}{2}\mathbf{C}\divideontimes\mathbf{C}-\mathbf{G}=\mathbf{0} && \text{in } \mathcal{B}_0, && (13f)\\
&\tfrac{1}{3}\mathbf{G}:\mathbf{C}-C=0 && \text{in } \mathcal{B}_0, && (13g)
\end{aligned}$$

which are accompanied by the boundary conditions

$$\begin{aligned}
&\boldsymbol{\varphi}=\bar{\boldsymbol{\varphi}} && \text{on } \partial_{\boldsymbol{\varphi}}\mathcal{B}_0,\\
&(2\mathbf{F}\boldsymbol{\Lambda}^{\mathbf{C}})\mathbf{N}=\bar{\mathbf{T}} && \text{on } \partial_{\boldsymbol{T}}\mathcal{B}_0,
\end{aligned} \qquad (14)$$

where $\bar{\boldsymbol{\varphi}}$ denotes the prescribed displacements on the Dirichlet boundary $\partial_{\boldsymbol{\varphi}}\mathcal{B}_0$ and $\mathbf{N}$ is the material outward normal vector to the Neumann boundary $\partial_{\boldsymbol{T}}\mathcal{B}_0$.

3 Electro-Thermo-Elastodynamics

In this section, we show how the mixed elastostatic framework from Sec. 2 can be transferred to the case of electro-thermo-elastodynamics. To this end, we first present the (initial) boundary value problems of thermodynamics and electrostatics. Then, we show how the different processes can be coupled using a suitable energy density function. Afterwards, we explain how the corresponding weak form can be derived, how an energy-momentum consistent temporal discretization can be obtained, and how the problem can be spatially discretized using the finite element method. Finally, a numerical example illustrates the advantageous properties of our novel framework.

3.1 Initial boundary value problem of thermodynamics

Thermodynamic problems can be described as initial boundary value problems. To facilitate the design of the energy-momentum consistent integration scheme, we employ the following version of the local energy balance as the governing differential equation, i.e.,

$$\theta\dot{\eta}+\mathrm{Div}\,\mathbf{Q}-\bar{R}=\frac{\mathrm{d}}{\mathrm{d}t}(\theta\eta)-\dot{\theta}\eta+\mathrm{Div}\,\mathbf{Q}-\bar{R}=0 \qquad \text{in } \mathcal{B}_0\times\mathcal{I}. \qquad (15)$$

This differential equation is accompanied by the boundary conditions

$$\begin{aligned}
&\theta=\bar{\theta} && \text{on } \partial_{\theta}\mathcal{B}_0\times\mathcal{I},\\
&\mathbf{Q}\cdot\mathbf{N}=-\bar{Q} && \text{on } \partial_{Q}\mathcal{B}_0\times\mathcal{I}
\end{aligned} \qquad (16)$$

and the initial condition

$$\theta(t=0)=\theta_0 \qquad \text{in } \mathcal{B}_0. \qquad (17)$$

In the above, θ is the absolute temperature field, η denotes the entropy density, $\mathbf{Q}$ represents the Piola heat flux vector, and $\bar{R}$ denotes a prescribed heat source. Moreover, $\bar{\theta}$ denotes the prescribed temperature field on the Dirichlet boundary $\partial_{\theta}\mathcal{B}_0$ and $\bar{Q}$ is a prescribed rate of heat transfer applied on the Neumann boundary $\partial_{Q}\mathcal{B}_0$. The initial boundary value problem is considered throughout the time interval $\mathcal{I}=[0,T]$, where $T\in\mathbb{R}^{+}$.

3.2 Boundary value problem of electrostatics

The electric processes within the capacitor-like DEAs can be described by a boundary value problem. This consists of the differential equations

$$\left.\begin{aligned}
&\mathrm{Div}(\mathbf{D}_0)=\bar{\rho}_0^{e}\\
&\mathbf{E}_0=-\nabla_{\mathbf{X}}\Phi
\end{aligned}\right\} \text{ in } \mathcal{B}_0, \qquad (18)$$

corresponding to Maxwell's equations, neglecting time-dependent and magnetic effects, and the associated boundary conditions

$$\begin{aligned} \Phi &= \bar{\Phi} && \text{on } \partial_\Phi \mathcal{B}_0, \\ \mathbf{D}_0 \cdot \mathbf{N} &= -\bar{\omega}_0^e && \text{on } \partial_\omega \mathcal{B}_0. \end{aligned} \tag{19}$$

Therein, $\mathbf{D}_0$ is the Lagrangian electric displacement vector, $\bar{\rho}_0^e$ denotes a prescribed electric volume charge, $\mathbf{E}_0$ represents the Lagrangian electric field vector, and Φ is the electric potential field which is prescribed with $\bar{\Phi}$ on the Dirichlet boundary $\partial_\Phi \mathcal{B}_0$. Furthermore, $\bar{\omega}_0^e$ denotes a prescribed electric surface charge on the Neumann boundary $\partial_\omega \mathcal{B}_0$.

3.3 Coupling via a suitable energy density function

To couple the mechanical, thermal, and electric processes governed by the aforementioned differential equations, we employ an energy density function inspired by the concept of polyconvexity (cf. [4]). More precisely, we consider an enhanced Mooney-Rivlin material model that describes the material behavior of the elastomer layer and can be additively decomposed according to

$$\psi(\mathbf{C}, \mathbf{G}, C, \mathbf{D}_0, \theta) = f_\theta(\theta)\,[\psi_{\mathrm{m}}(\mathbf{C}, \mathbf{G}, C) + \psi_{\mathrm{em}}(\mathbf{C}, C, \mathbf{D}_0)] + \psi_{\mathrm{t}}(\theta) + \psi_{\mathrm{tm}}(C, \theta). \tag{20}$$

The utilization of this energy density function ψ leads to a fully coupled formulation, as it couples mechanical $(\mathbf{C}, \mathbf{G}, C)$, electric $(\mathbf{D}_0)$, and thermal quantities (θ) with each other. For the chosen energy density function, the constitutive laws

$$\eta = -\partial_\theta \psi, \quad \mathbf{E}_0 = \partial_{\mathbf{D}_0} \psi \tag{21}$$

are valid. Furthermore, assuming thermal isotropy, we obtain the Piola heat flux vector by

$$\mathbf{Q} = -k_0 C^{-1} \mathbf{G} \nabla_{\mathbf{X}} \theta, \tag{22}$$

where k_0 is the coefficient of thermal conductivity.

3.4 Derivation of the weak form and temporal discretization using an energy-momentum scheme

The merged (initial) boundary value problems of electrostatics, thermodynamics, and elastostatics form the basis for the final mixed initial boundary value problem of electro-thermo-elastodynamics, which describes the behavior of DEAs. However, to account for dynamic effects, we extend the balance of linear momentum (13a) with the inertia term. Moreover, we employ the energy density function (20) and the related constitutive equations to achieve coupling between the different physical processes.

It is possible to derive the weak form of this final mixed initial boundary value problem by multiplying the underlying equations with test functions, integrating over the domain $\mathcal{B}_0$, and using basic algebraic operations. Following this standard procedure, we obtain, for example, the weak form for (13c) as

$$\int_{\mathcal{B}_0} \mathbf{w}_{\mathbf{G}} : \left(\partial_{\mathbf{G}} \psi - \mathbf{\Lambda}^{\mathbf{G}} + \frac{1}{3} \Lambda^C \mathbf{C} \right) \mathrm{d}V = 0. \tag{23}$$

The weak form can then be discretized in time, which we again show only for (23), i.e., we propose

$$\int_{\mathcal{B}_0} \mathbf{w}_{\mathbf{G}} : \left(\mathrm{D}_{\mathbf{G}} \psi - \mathbf{\Lambda}^{\mathbf{G}}_{n+1} + \frac{1}{3} \Lambda^C_{n+1} \mathbf{C}_{n+\frac{1}{2}} \right) \mathrm{d}V = 0. \tag{24}$$

Our chosen temporal discretization of the weak form is special in that it can be shown to be energy and momentum consistent. Thereby, the energy consistency is essentially due to the properties of the so-called discrete or algorithmic derivatives $\mathrm{D}_{(\bullet)}\psi$, which we use in the sense of Gonzalez [6] in our work. Moreover, our chosen temporal discretization yields a one-step method that is second-order accurate and stable even for large time step sizes.

3.5 Spatial discretization: Finite element method

For the spatial discretization, we employ the finite element method. More specifically, in the upcoming numerical example we use hexahedral elements, following a standard isoparametric (Bubnov) Galerkin approach. We discretize the unknown fields $\boldsymbol{\varphi}$, θ, and Φ using 20-node serendipity shape functions. For the remaining quantities $\mathbf{D}_0$, $\mathbf{\Xi}$, and $\mathbf{\Lambda}$, we use 8-node Lagrangian shape functions. It is worth mentioning that the latter quantities do not have to be continuous over the element boundaries and can therefore be eliminated by a static condensation procedure. This enables an efficient computation despite the large number of unknowns.

3.6 Numerical example

In this section, we illustrate the properties of our novel mixed framework with a numerical example. More precisely, we investigate the L-shaped block, given in Fig. 1 with its initial geometry, mesh, and temperature distribution. The body can move freely in space and is only subjected to the electrical Dirichlet boundary conditions

$$\bar{\Phi}(X_1, X_2, X_3 = 0, t) = \begin{cases} 6\,\sin(\frac{\pi t}{10}\,\frac{1}{\mathrm{s}}) & \text{for } t < 5\,\mathrm{s} \\ 6 & \text{for } t \geq 5\,\mathrm{s} \end{cases} \mathrm{MV}, \quad \bar{\Phi}(X_1, X_2, X_3 = 1.5\,\mathrm{m}, t) = 0 \tag{25}$$

and the mechanical Neumann boundary conditions

$$\bar{\mathbf{T}}(X_1, X_2 = 10\,\mathrm{m}, X_3, t) = f(t) \begin{pmatrix} 256/9 \\ 512/9 \\ 768/9 \end{pmatrix} \mathrm{Pa}, \quad \bar{\mathbf{T}}(X_1 = 6\,\mathrm{m}, X_2, X_3, t) = -f(t) \begin{pmatrix} 256/9 \\ 512/9 \\ 768/9 \end{pmatrix} \mathrm{Pa}, \tag{26}$$

with

$$f(t) = \begin{cases} t\,\frac{1}{\mathrm{s}} & \text{for } t < 2.5\,\mathrm{s} \\ 5 - t\,\frac{1}{\mathrm{s}} & \text{for } 2.5\,\mathrm{s} \leq t < 5\,\mathrm{s}\,. \\ 0 & \text{for } t \geq 5\,\mathrm{s} \end{cases} \tag{27}$$

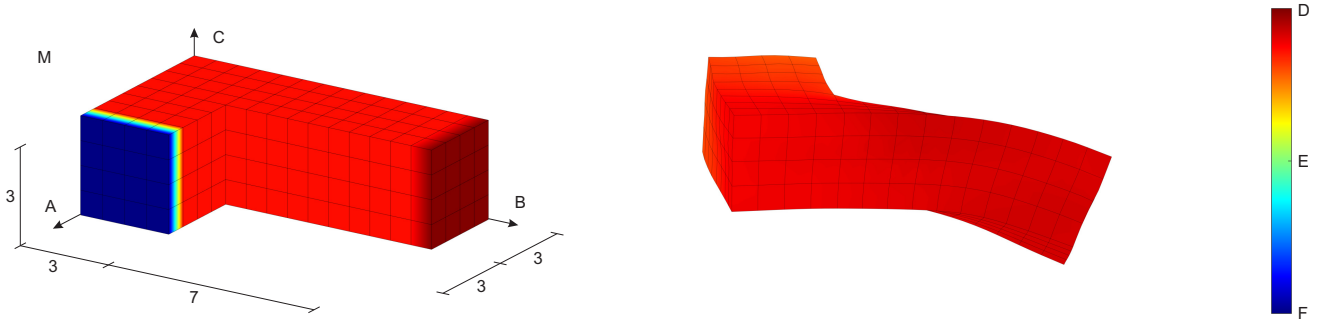

Fig. 1: Left: The L-shaped block with its initial geometry, mesh, and temperature distribution θ_0 [K]. Right: The L-shaped block at $t = 40\,\mathrm{s}$.

The body is simulated for a total time $T = 40\,\mathrm{s}$ using a time step size $\Delta t = 1\,\mathrm{s}$. As can be seen from the definition of the loads, the simulation can be divided into two phases. After the body has undergone strong nonlinear deformation during a first phase, the load phase, in which $t < 5\,\mathrm{s}$, no external forces are present anymore for $t \geq 5\,\mathrm{s}$. Therefore, we can expect both the total angular momentum as well as the total energy to be conserved in the second phase. As Figs. 2 and 3 show, the proposed formulation using an EM scheme is indeed able to consistently reproduce this physical requirement. That this is not a self-evident property can be seen by comparing the proposed formulation with other methods for the temporal discretization, for example, with the midpoint rule (MP). As can be seen in Fig. 3, using this method results in an energy blow-up, meaning that physically wrong results are computed and the simulation is aborted.

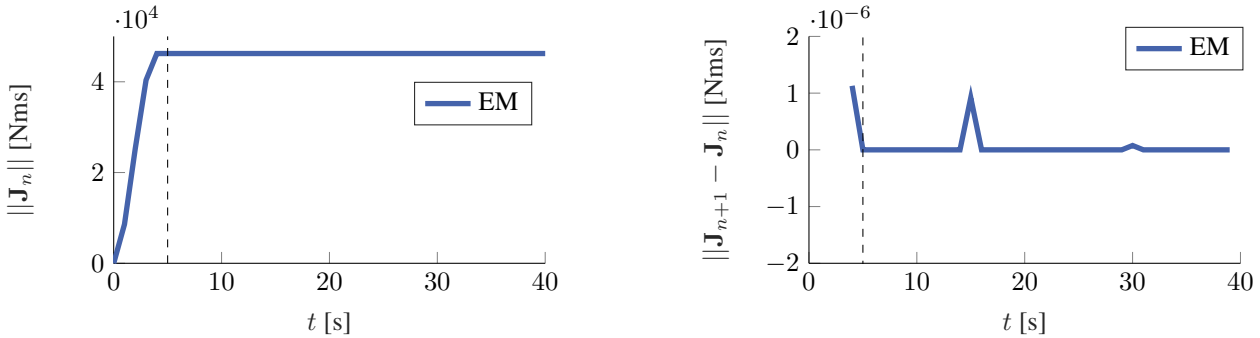

Fig. 2: Left: Evolution of the total angular momentum computed using the proposed energy-momentum scheme (EM). Right: Incremental changes of the total angular momentum from one time step to the next when using the EM.

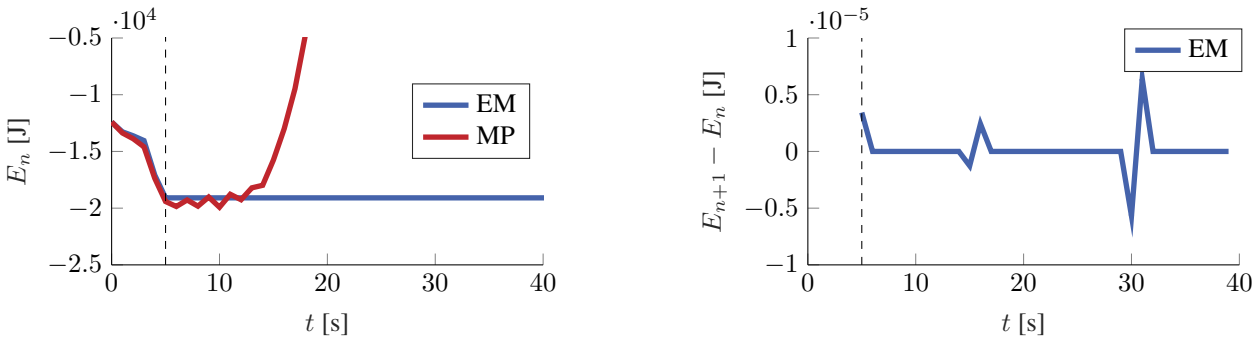

Fig. 3: Left: Evolution of the total energy computed using both the proposed energy-momentum scheme (EM) and the midpoint rule (MP). Right: Incremental changes of the total energy from one time step to the next when using the EM.

4 Conclusion

In summary, we have developed a novel mixed formulation for the simulation of electro-thermo-elastodynamic systems, in particular of dielectric elastomer actuators. We first introduced a mixed framework for elastostatics that we subsequently extended to the case of electro-thermo-elastodynamics. The path we have pointed out is very general and can be similarly applied to a variety of other problems. Furthermore, we have indicated how such systems can be treated numerically. In this context, we have explained how an energy-momentum consistent temporal discretization can be conducted. Using a suitable spatial discretization, we were eventually able to illustrate the advantageous properties of our novel framework in a numerical example. We would like to point out that a publication is currently under preparation that will address this novel framework in more detail [7].

Acknowledgements Our thanks go to Moritz Hille, M.Sc., for his expertise and support. In addition, we gratefully acknowledge the financial support provided by the Deutsche Forschungsgemeinschaft (DFG) - project number 443238377. Open access funding enabled and organized by Projekt DEAL.

References

[1] C. Majidi, Advanced Materials Technologies **4**(2), 1800477 (2019).
[2] J. Bonet, A. J. Gil, and R. Ortigosa, Computer Methods in Applied Mechanics and Engineering **283**, 1061–1094 (2015).
[3] P. Betsch, A. Janz, and C. Hesch, Computer Methods in Applied Mechanics and Engineering **335**, 660–696 (2018).
[4] M. Franke, R. Ortigosa, J. Martínez-Frutos, A. Gil, and P. Betsch, Computer Methods in Applied Mechanics and Engineering **389**, 114298 (2022).
[5] J. M. Ball, Archive for Rational Mechanics and Analysis **63**(4), 337–403 (1976).
[6] O. Gonzalez, Journal of Nonlinear Science **6**(5), 449–467 (1996).
[7] M. Franke, F. Zähringer, M. Hille, R. Ortigosa, and P. Betsch, in preparation (2022).